UC Berkeley

Title

Oxidative cyclization of prodigiosin by an alkylglycerol monooxygenase-like enzyme

Authors

de Rond, Tristan
Stow, Parker
Eigl, Ian
et al.

Peer reviewed

Oxidative cyclization of prodigiosin by an alkylglycerol monooxygenase-like enzyme

Tristan de Rond[1]* , Parker Stow[1], Ian Eigl[2], Rebecca E Johnson[1], Leanne Jade G Chan[3,4], Garima Goyal[3,4], Edward E K Baidoo[3,4], Nathan J Hillson[3–5], Christopher J Petzold[3,4] , Richmond Sarpong[1] & Jay D Keasling[2–4,6,7]*

Prodiginines, which are tripyrrole alkaloids displaying a wide array of bioactivities, occur as linear and cyclic congeners. Identification of an unclustered biosynthetic gene led to the discovery of the enzyme responsible for catalyzing the regiospecific C–H activation and cyclization of prodigiosin to cycloprodigiosin in *Pseudoalteromonas rubra*. This enzyme is related to alkylglycerol monooxygenase and unrelated to RedG, the Rieske oxygenase that produces cyclized prodiginines in *Streptomyces*, implying convergent evolution.

The prodiginines are a family of red tripyrrole natural products that display a broad range of promising medicinal properties, including antimalarial, anticancer, and immunosuppressive activities[1–3]. Notably, they have been shown to induce apoptosis in cancer cells while leaving nonmalignant cells unaffected[3–5]. Most prodiginines occur in linear and cyclic forms with respect to their aliphatic tails, which is apparent when comparing the structures of prodigiosin (**1**) to cycloprodigiosin (**2**), and undecylprodigiosin to streptorubin B (**Fig. 1**). It has been proposed that these carbocycles bias the molecules toward their biologically active conformations[6]. For instance, the cyclic prodiginine **2** was found to be more potent against a variety of bacteria than **1**, its straight-chain congener[7].

The biosynthesis of cyclic prodiginines involves oxidative cyclization of their respective linear congeners (**Fig. 1a**). The enzymes catalyzing the cyclization reactions to produce streptorubin B, metacycloprodigiosin, marineosin, and roseophilin in various *Streptomyces* spp. all belong to a family of Rieske oxygenases represented by *Streptomyces coelicolor* RedG (**Fig. 1c**)[8–11]. The catalytic capacities of these enzymes have been employed to synthesize natural and unnatural cyclic prodiginines[10–12]. However, to date, no enzyme catalyzing the cyclization of **1** into **2** has been identified. Given the difficulty of realizing regiospecific C–H activation using traditional synthetic methods, additional enzymes catalyzing such oxidative cyclizations would be a welcome expansion of the biocatalytic toolbox. Here, we identify the enzyme responsible for the regiospecific C–H activation and cyclization of **1** in *P. rubra*, which is known to produce both **1** and **2**. This enzyme is unrelated to RedG, but is rather a member of the fatty acid (FA) hydroxylase integral membrane di-iron oxygenase family (Pfam PF04116), and is closely related to metazoan alkylglycerol monooxygenase.

In *Serratia* spp., the *pig* ('pigment') gene cluster encodes the enzymes responsible for biosynthesis of **1** (refs. 13,14). Apart from *pigK* and *pigN*, whose precise roles remain uncharacterized, the function of each *pig* gene has been elucidated. The biosynthesis of **1** proceeds through a bifurcated pathway (**Fig. 1a**). PigBDE

biosynthesize 2-methyl-3-amylpyrrole (MAP, **3**). PigA and PigF–N form 4-methoxy-2,2′-bipyrrole-5-carboxaldehyde (MBC, **4**), and PigC condenses these two intermediates to yield **1**. We expected the biosynthesis of **1** to proceed in a similar manner in *P. rubra*, given that its genome[15] harbors a biosynthetic cluster showing high sequence identity with the *Serratia* ATCC39006 *pig* cluster (**Fig. 1b** and **Supplementary Results**, **Supplementary Table 1**).

To ensure that cyclization is the final step in cyclic prodiginine biosynthesis in *P. rubra*, as is the case in *S. coelicolor*[8] (**Fig. 1c**), we constructed an in-frame Δ*pigE* mutant of *P. rubra*. As expected, this mutant produced neither **1** nor **2**, but upon feeding **1**, we detected **2** using LC–MS (**Supplementary Fig. 1**). These results confirmed that the cyclization of **1** in *P. rubra*, like that in *S. coelicolor*, can occur as the final step in **2** biosynthesis. Further support for this model is the observation that recombinant *Escherichia coli* expressing *P. rubra pigBCDE* produces **1** but not **2** upon feeding with synthetic **4** (**Fig. 2a** and **Supplementary Fig. 2**).

Bioinformatic analysis of the *P. rubra* genome[15] revealed no *redG* homologs, and the only genes encoding enzymes homologous to oxidases found in the *pig* cluster were those already ascribed to steps in the **1** biosynthesis pathway. Upon examining the *P. rubra pig* cluster for genes not present in *Serratia* (which does not produce **2**), we noticed that although the two clusters show near-perfectly conserved synteny, the *P. rubra* cluster actually lacks a *pigN* gene (**Fig. 1b**). Although we found no close *pigN* homolog in the *P. rubra* genome, we did detect a homolog of *S. coelicolor redF*, which is thought to fulfill the role of *pigN* in *S. coelicolor*[13,14] in the *PRUB675* locus. (For a more in-depth analysis of the relationship between these proteins, which are all in the DUF1295 protein family, see **Supplementary Fig. 3**.) In *Serratia*, disruption of *pigN* impedes, but does not abolish, conversion of 4-hydroxy-2,2′-bipyrrole-5-carboxaldehyde (HBC, **5**) into **4**. Accumulation of **5** results in diminished production of **1** and increased production of norprodigiosin (**6**), which is formed by the PigC-catalyzed condensation of **5** with **3** (ref. 16). The same phenotype was observed for *P. rubra* Δ*PRUB675*, suggesting that *PRUB675* fulfills the function of *pigN* in *P. rubra* (**Supplementary Fig. 4**).

The gene neighborhood of *PRUB675* revealed that the gene appears to be part of a transcriptional unit with *PRUB680*, which bears homology to di-iron oxygenases. Deleting *PRUB680* in *P. rubra* abolished production of **2**, but had no effect on **1** (**Fig. 2a**). Furthermore, heterologous expression of *PRUB680* alongside *pigBCDE* in *E. coli* fed **4** led to the formation of **2**. Direct bioconversion of **1** to **2** by recombinant *E. coli* could barely be observed, which has also been the case for the bioconversion of undecylprodigiosin to
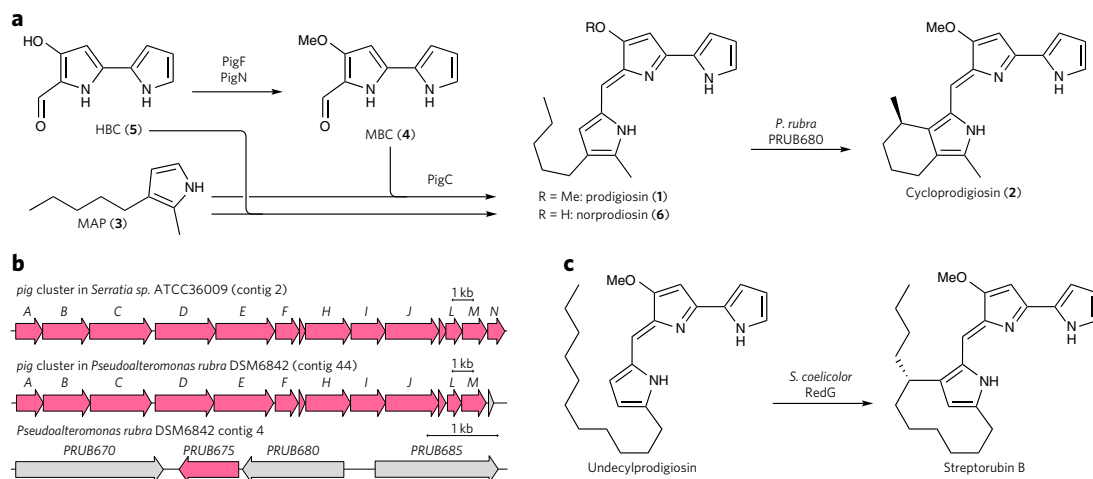
Figure 1 | Biosynthesis of prodiginines in *P. rubra* compared to that in other organisms. (a) Hypothetical prodigiosin (**1**) biosynthetic pathway in *P. rubra* (analogous to the pathway elucidated in *Serratia*) and the cyclization of **1** into cycloprodigiosin (**2**) investigated in this work. (**b**) Comparison of the *pig* gene clusters in *Serratia*, which produces only **1**, and *P. rubra*, which produces both **1** and **2**, shows that *pigN* is absent in the latter. The gene downstream of *pigM* in *P. rubra* shows no similarity to *pigN*. Also shown is an excerpt of *P. rubra* contig 4, which contains *PRUB675* and *PRUB680*. Genes in pink have homology to *Serratia pig* genes and/or to *Streptomyces red* genes. (**c**) The Rieske monooxygenase-like RedG catalyzes the carbocyclization of undecylprodigiosin to form streptorubin B, motivating our search for the enzyme responsible for the analogous cyclization of **1** in *P. rubra*.

streptorubin B by *Streptomyces* expressing *redG*[8]. We suspect that **1** is unable to cross the *E. coli* cell wall effectively, whereas **4** can.

Bioinformatic analysis showed that PRUB680 shares no substantial sequence similarity with RedG and is instead a member of the FA hydroxylase family of integral membrane di-iron oxygenases. PRUB680 displays the characteristic eight-histidine motif that is essential for iron binding and catalysis in this enzyme family (**Supplementary Fig. 5**)[17,18]. Di-iron oxygenases are known to carry out a wide variety of C–H activation chemistries (**Supplementary Figs. 6** and **7**; **Supplementary Table 2**)[17], but so far none have been reported to catalyze oxidative cyclization or C–C bond formation[19].

The closest characterized homolog of PRUB680 is alkylglycerol monooxygenase (AGMO), which is present only in metazoans and some protists and forms an isolated eukaryotic branch of the FA hydroxylase family. AGMO plays a central role in lipid homeostasis by catalyzing the breakdown of ether lipids, a deficit of which leads to the development of cataracts and disrupts spermatogenesis in mice[20]. AGMO is distinct among di-iron oxygenases—most of which obtain their reducing equivalents from nicotinamide cofactors—in that it utilizes pterin cofactors, which are thought to bind in a pocket on the cytosolic side of this transmembrane protein[21]. To ensure that a possible analogous pocket in PRUB680 would be accessible to exogenously added reducing cofactors, we pursued the *in vitro* characterization of PRUB680 in inverted membrane vesicles generated via sonication of *E. coli* spheroplasts[22]. Under these conditions, we were able to observe PRUB680-catalyzed conversion of **1** to **2**. Like AGMO, PRUB680 appeared to require pterin cofactors to supply its reducing equivalents, accepting various pterins equally well (**Fig. 2b**); nicotinamide and flavin cofactors were not accepted.

PRUB680 was inhibited by EDTA, but activity could be recovered by iron supplementation (**Fig. 2b**), suggesting that, like all other characterized members of the FA hydroxylase family, PRUB680 utilizes iron to achieve catalysis. Copper and vanadium—other metals known to facilitate enzymatic C–H activation[19]—could not recover activity. Based on the mechanistic analysis of other di-iron enzymes[17,18], we propose that the cyclization of **1** proceeds by abstraction of an aliphatic hydrogen followed by addition of the radical into the tripyrrole π system (**Supplementary Fig. 8**).

Besides the functional similarity between PRUB680 and AGMO, the catalytic domains of these enzymes share 43% sequence identity (**Supplementary Fig. 9**) and are predicted to have the same

nine-transmembrane topology (**Supplementary Fig. 5**)[21]. Because all efforts to express AGMO in microbial hosts have thus far been unsuccessful[20,23], PRUB680 may serve as a convenient model system for the biochemical characterization of this enzyme.

PRUB680 resides in a predominantly prokaryotic clade of the FA hydroxylase protein family (**Supplementary Fig. 6**), which, considering the remarkable catalytic diversity displayed by the few members characterized thus far, may contain many enzymes catalyzing novel C–H activation reactivity. Moreover, some of these unexplored enzymes may be involved in C–H activating steps in the biosynthesis of novel natural products. None of PRUB680's closest homologs are found in organisms known to produce prodiginines (**Supplementary Fig. 7**), suggesting that PRUB680 is a functional outlier among enzymes that carry out other oxidative chemistry. The genomic context of these homologs of PRUB680 gives no clear indication regarding their functions (**Supplementary Table 3**).

Most characterized bacterial biosynthetic pathways are encoded by genes that are physically clustered on the genome[20]. However, in *P. rubra*, the genes encoding prodiginine biosynthesis are split across two loci, a situation we were alerted to by the absence of the strictly conserved gene *pigN*. An analogous strategy may help to identify biosynthetic enzymes in other organisms that are not clustered with their respective pathways.

The exact role of PigN in prodiginine biosynthesis is still unknown. Given that PigB, which catalyzes the final step of **3** biosynthesis, is predicted to have two transmembrane helices (**Supplementary Fig. 10**), and PigC has been found to localize to the membrane when expressed heterologously[24], we suspect that the concluding steps of **1** biosynthesis occur at the membrane. PigN has five predicted transmembrane helices (**Supplementary Fig. 11**) and may act to recruit PigF to the membrane. The presence of *pigN* (or *redF*) is strictly conserved among prodiginine-producing organisms despite the weak phenotype of Δ*pigN* merely decreasing the ratio of **1** to **6**, but not abolishing **1** production. *P. rubra* may have acquired *pigA–M* in one horizontal gene transfer event while acquiring *PRUB675–680* independently, perhaps due to strong selective pressure for a gene fulfilling the role of *pigN*.

In summary, we have shown that PRUB680, a membrane di-iron oxygenase-like enzyme, produces **2** by cyclization of **1**, analogously to the cyclization of undecylprodigiosin to form streptorubin B catalyzed by RedG, a Rieske oxygenase-like enzyme. Despite sharing no
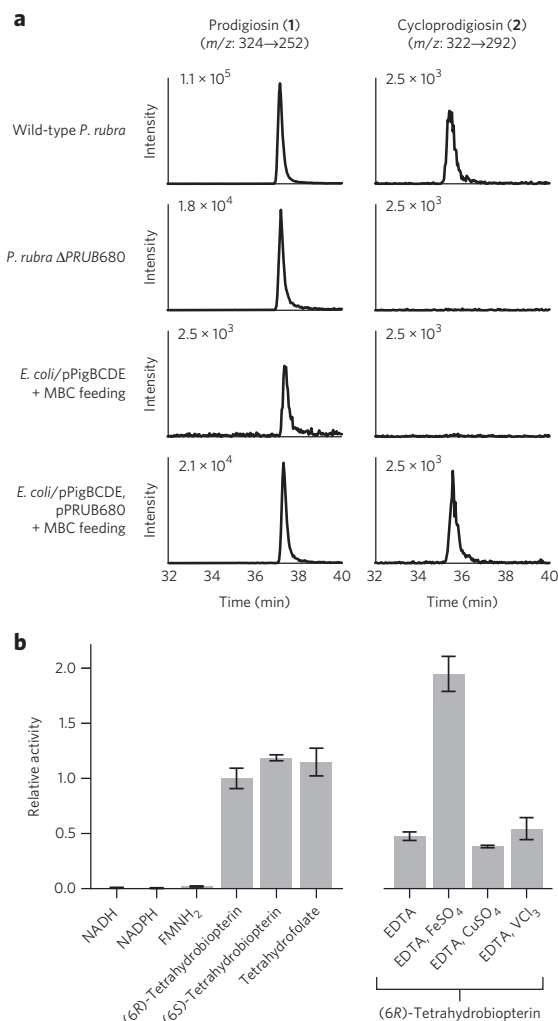
Figure 2 | Analysis of prodigiosin cyclization *in vivo* and *in vitro*. (**a**) *In vivo* production of prodiginines. In *E. coli*, the cells were fed MBC (**4**), which is turned into prodigiosin (**1**, left) by PigBCDE. **1** is in turn converted to cycloprodigiosin (**2**, right) by PRUB680 when present. For standards, see **Supplementary Figure 1**. p, plasmid. (**b**) *In vitro* experiments with PRUB680 in inverted *E. coli* membrane vesicles. Vesicles were shaken with **1** in the presence of the indicated cofactors (left). Reactions were initiated by addition of reducing cofactor. For metal dependency experiments (right), vesicles were incubated with EDTA, followed by metal ion, before initiating the reaction with (6*R*)-tetrahydrobiopterin. Error bars represent s.d. of triplicate *in vitro* assays using the same membrane vesicle preparation.

sequence similarity, both enzymes are predicted to employ histidine-ligated nonheme iron centers[18,25] to catalyze the oxidative cyclization of prodiginines. PRUB680 bears strong homology to AGMO and has similar cofactor requirements, and therefore may serve as a prokaryotic model for the latter. Furthermore, the uncharacterized bacterial enzymes related to PRUB680 may provide a valuable source of novel C–H activation reactivity. PRUB680 itself may also prove useful as a biocatalyst to produce novel prodiginines. The fact that cyclic prodiginine biosynthesis evolved independently at least twice suggests that there exists a strong selective pressure to produce cyclic prodiginines. However, thus far, the ecological role of the prodiginines—and hence the adaptive advantage conferred by cyclic prodiginines—remains an enigma.

Methods

Methods, including statements of data availability and any associated accession codes and references, are available in the online version of the paper.

References

1. Papireddy, K. *et al. J. Med. Chem.* **54**, 5296–5306 (2011).
2. Stankovic, N., Senerovic, L., Ilic-Tomic, T., Vasiljevic, B. & Nikodinovic-Runic, J. *Appl. Microbiol. Biotechnol.* **98**, 3841–3858 (2014).
3. Williamson, N.R. *et al. Future Microbiol.* **2**, 605–618 (2007).
4. Montaner, B. & Pérez-Tomás, R. *Life Sci.* **68**, 2025–2036 (2001).
5. Yamamoto, C. *et al. Hepatology* **30**, 894–902 (1999).
6. Jones, B.T., Hu, D.X., Savoie, B.M. & Thomson, R.J. *J. Nat. Prod.* **76**, 1937–1945 (2013).
7. Lee, J.S. *et al. Appl. Environ. Microbiol.* **77**, 4967–4973 (2011).
8. Sydor, P.K. *et al. Nat. Chem.* **3**, 388–392 (2011).
9. Salem, S.M. *et al. J. Am. Chem. Soc.* **136**, 4565–4574 (2014).
10. Withall, D.M., Haynes, S.W. & Challis, G.L. *J. Am. Chem. Soc.* **137**, 7889–7897 (2015).
11. Kimata, S., Izawa, M., Kawasaki, T. & Hayakawa, Y. *J Antibiot. (Tokyo)* **70**, 196–199 (2017).
12. Kancharla, P., Lu, W., Salem, S.M., Kelly, J.X. & Reynolds, K.A. *J. Org. Chem.* **79**, 11674–11689 (2014).
13. Hu, D.X., Withall, D.M., Challis, G.L. & Thomson, R.J. *Chem. Rev.* **116**, 7818–7853 (2016).
14. Williamson, N.R., Fineran, P.C., Leeper, F.J. & Salmond, G.P.C. *Nat. Rev. Microbiol.* **4**, 887–899 (2006).
15. Xie, B.-B. *et al. J. Bacteriol.* **194**, 1637–1638 (2012).
16. Williamson, N.R. *et al. Mol. Microbiol.* **56**, 971–989 (2005).
17. Shanklin, J., Guy, J.E., Mishra, G. & Lindqvist, Y. *J. Biol. Chem.* **284**, 18559–18563 (2009).
18. Bai, Y. *et al. Nature* **524**, 252–256 (2015).
19. Tang, M.-C., Zou, Y., Watanabe, K., Walsh, C.T. & Tang, Y. *Chem. Rev.* **117**, 5226–5333 (2017).
20. Watschinger, K. & Werner, E.R. *IUBMB Life* **65**, 366–372 (2013).
21. Watschinger, K. *et al. Biochem. J.* **443**, 279–286 (2012).
22. Futai, M. *J. Membr. Biol.* **15**, 15–28 (1974).
23. Mayer, M. *et al. Pteridines* **24**, 105–109 (2013).
24. Chawrai, S.R., Williamson, N.R., Mahendiran, T., Salmond, G.P.C. & Leeper, F.J. *Chem. Sci.* **3**, 447–454 (2012).
25. Barry, S.M. & Challis, G.L. *ACS Catal.* **3**, 2362–2370 (2013).

Author contributions

T.d.R., R.E.J., R.S., and J.D.K. conceived of the study. T.d.R., P.S. and I.E. constructed plasmids and performed microbiological manipulations and extractions, R.E.J. performed synthetic organic chemistry. T.d.R., E.E.K.B., and C.J.P. performed analytical chemistry, L.J.G.C. and C.J.P. performed proteomic analysis, and G.G. and N.J.H. PCR amplified and purified DNA fragments. T.d.R. performed bioinformatic analysis. All authors contributed to the manuscript.

Competing financial interests

The authors declare no competing financial interests.

Additional information

Any supplementary information, chemical compound information and source data are available in the online version of the paper. Reprints and permissions information is available online at http://www.nature.com/reprints/index.html. Publisher's note: Springer Nature remains neutral with regard to jurisdictional claims in published maps and institutional affiliations. Correspondence and requests for materials should be addressed to T.d.R. or J.D.K.

ONLINE METHODS

Synthetic chemistry. Cycloprodigiosin (2)[26] and MBC (4)[27] were synthesized as described previously.

Bacterial cultivation. *E. coli* was propagated at 37 °C on LB agar or in LB medium. For the cultivation of *P. rubra* (at 30 °C), these media were supplemented with 10% v/v 180 g/L Instant Ocean Sea Salt (IO; Spectrum Brands, Blacksburg, VA) and autoclaved separately. Descriptions of bacterial strains employed in this study are provided in **Supplementary Table 4**.

Plasmid construction. DNA assembly protocols were designed using j5 and DeviceEditor software[28]. Descriptions of plasmids employed in this study are provided in **Supplementary Table 5**. Assembly of DNA fragments (**Supplementary Table 6**) was performed using NEBuilder HiFi DNA Assembly Master Mix or NEB Golden Gate Assembly Mix (NEB) per the manufacturer's directions. The 11-kb *pigBCDE* fragment was cloned behind a T7 promoter using the Zero Blunt TOPO PCR Cloning Kit (Thermo Fisher).

Targeted gene disruptions in *P. rubra*. We employed conjugative transfer of a suicide plasmid following literature precedent[29]; however, counterselection with SacB was not effective in our hands. This held true even with *sacB* under the control of promoters expressed highly in *P. rubra*, as determined by shotgun proteomics (**Supplementary Table 7**). Instead, we replaced *sacB* with *lacZ* and identified double crossovers by blue–white screening (**Supplementary Fig. 12**). *E. coli* WM3064 was transformed with suicide vectors conferring both erythromycin and chloramphenicol resistance markers under the control of the *P. rubra* elongation factor G (*PRUB9669* on contig 67) promoter, the *P. rubra* 30S ribosomal protein S13 promoter (*PRUB13406* on contig 115; this is actually a polycistronic locus with a number of ribosomal proteins and an RNA polymerase subunit) driving *lacZ*, and ~1 kb regions homologous to those upstream and downstream of the target. After overnight growth on LB agar with 25 µg/mL chloramphenicol, 100 µM X-gal, and 300 µM diaminopimelic acid (DAP), a colony was patched directly on LB agar with 4% v/v 180 g/L IO and 300 µM DAP, with a wild-type *P. rubra* colony patched on top. After conjugating at 30 °C overnight, the patch was struck out for single colonies on LB agar with 10% v/v 180 g/L IO, 25 µg/mL erythromycin, and 500 µM X-gal. Blue colonies (single-crossovers) were passaged until homogeneous. These were then subcultured on the same growth media without erythromycin, and white colonies were isolated and confirmed to be sensitive to erythromycin. To distinguish double crossovers from revertants, colony PCR was performed by picking colonies into neat DMSO, diluting 1:10 with water and using that as template (1% v/v) with 5Prime HotMasterMix polymerase and primers as specified in **Supplementary Table 6**.

Prodiginine production in *P. rubra*. *P. rubra* was grown in 50 mL 20% v/v LB, 10% v/v 180 g/L IO, and 70% de-ionized water in a 250-mL baffled shake flask. After 12 h of growth at 30 °C, 2 mL of the culture was extracted with 3 mL 1:1 chloroform:methanol. The organic layer was evaporated to dryness, dissolved in ethanol, diluted 1:1 in de-ionized water, and analyzed by LC–MRM–MS and LC–TOF–MS.

Heterologous prodiginine production in *E. coli*. *E. coli* BLR (DE3) was transformed with plasmids containing *pigBCDE* and either *PRUB680* or RFP. Overnight cultures were diluted 1:10 into LB medium supplemented with 50 µg/mL kanamycin and 25 µg/mL chloramphenicol and grown at 37 °C to an optical density at 600 nm (OD$_{600}$) of 0.6, upon which they were induced with 100 µM IPTG at 30 °C for 16 h. 10 mL of cells were harvested by centrifugation (8,000g for 5 min), resuspended in 300 µL of LB medium, and spread onto agar plates with 0.1 mM IPTG and antibiotics as before. 10 µL of 1 mM MBC in 1:3 DMSO:water was spotted onto the plates, which were left to grow overnight at 30 °C. The pink halo (as can be seen in **Supplementary Fig. 2**) was scraped off and resuspended in 1 mL de-ionized water with 2% TFA by vigorous vortexing. The cell suspension was extracted with 2 mL of 1:1 v/v chloroform:methanol. The organic layer was evaporated to dryness dissolved in ethanol, diluted 1:1 in de-ionized water, and analyzed by LC–MRM–MS.

***In vitro* analysis of PRUB680 in inverted *E. coli* membrane vesicles.** An overnight culture of *E. coli* BLR (DE3) containing pET28-PRUB680 was diluted 1:10 into 3 × 500 mL LB medium supplemented with 50 µg/mL kanamycin in 2-L baffled flasks and grown at 37 °C. When the cells reached an OD$_{600}$ of 0.6, the flasks were cooled to 18 °C and induced with 100 mM IPTG for 3 h. The cells were harvested by centrifugation (5,000g for 10 min), washed with 30 mL spheroplasting buffer (30% sucrose, 200 mM Tris–HCl pH 8.0, 2 mM EDTA) and incubated, rocking for 30 min at room temperature in 30 mL spheroplasting buffer + 3 mg lysozyme. Spheroplasts were harvested by centrifugation (5,000g for 10 min), resuspended in 30 mL assay buffer (100 mM HEPES–KOH pH 7.8, 50 mM K$_2$SO$_4$, 1% v/v Sigma Protease Inhibitor Cocktail P8849), divided into 20 × 1.5 mL in 2-mL centrifuge tubes, and sonicated in a cup-horn sonicator (Qsonica Q700 with 431MPX horn; amplitude: 75%, 1 min on, 1 min off) for 45 min. of total 'on' time. The water bath temperature was maintained between 3 and 10 °C. The tubes were centrifuged at 12,000g for 10 min at 4 °C, and the supernatants were then combined and again centrifuged at 12,000g for 10 min at 4 °C. The supernatant was centrifuged at 120,000g for 30 min at 4 °C, and the orange pellet thoroughly resuspended in 22 mL assay buffer. For each reaction, 500 µL of the vesicle preparation was used. For the metal dependence experiments, EDTA was added to a final concentration of 4 mM, and the mixture was incubated at 4 °C for 5 min, followed by the addition of metal at a concentration of 5 mM and incubation at 4 °C for 5 min. For all experiments, 10 µM prodigiosin (Enzo Life Sciences, 100× stock solution prepared at 1 mM in 20% v/v ethanol in water) was added, the mixture transferred to a round-bottom glass tube (16 mm × 100 mm) at room temperature. The reaction was started by adding reducing cofactor (NADH, NADPH, (6*R*)- or (6*S*)-tetrahydrobiopterin, or tetrahydrofolate, all from Sigma-Aldrich) at 250 µM, or, in the case of FMNH$_2$, adding flavin mononucleotide (FMN) to the mixture preloaded with a cofactor generation system consisting of 20 mM glucose-6-phosphate, 250 µM NADP$^+$, 1 unit/mL glucose-6-phosphate dehydrogenase, and 1 unit/mL NADPH:FMN oxidoreductase from *Photobacterium fischeri* (all from Sigma-Aldrich). Enzymatic generation of FMNH$_2$ was necessary, because PRUB680 is inactivated by sodium dithionite. The *in situ* reduction of FMN to FMNH$_2$ was verified by observing the loss of yellow color. Metal dependence experiments used 250 µM (6*R*)-tetrahydrobiopterin. After shaking at 200 r.p.m. at room temperature for 10 min, reactions were quenched using 2 mL 1:1 v/v chloroform:methanol. 500 µL de-ionized water was added, and the organic layer evaporated to dryness, dissolved in ethanol, diluted 1:1 with de-ionized water, and analyzed by LC–MRM–MS. Peak areas were calculated using Analyst 1.6.2. To calculate relative enzyme activity, cycloprodigiosin peak areas were normalized to the prodigiosin starting material peak areas to correct for extraction efficiency (<0.1% conversion had occurred under all conditions), and to a (6*R*)-tetrahydrobiopterin reaction to normalize for enzyme activity differences between vesicle preparations. All conditions shown in **Figure 2b**, except for FMNH$_2$, were performed in parallel with the same vesicle preparation.

LC–MS acquisition and data analysis. LC–MRM–MS was performed on an AB Sciex 4000 QTRAP with an Agilent 1200 series LC system. 1 µL of sample was injected onto a Phenomenex Kinetex XB-C18 (3 mm × 100 mm) column. Mobile phase: A = 10 mM ammonium formate, brought to pH 4.5 with formic acid; B = methanol buffered identically to A. Method: 35% B for 5 min, ramp from 35% to 80% B in 30 min, 80% B for 8 min, ramp to 35% B in 2 min, re-equilibrate at 35% B for 15 min; all at a flow rate of 200 µL/min. A Turbo Spray V ion source was used in positive ion mode (curtain gas: 20 L/min; temperature: 600 °C; voltage: 4,800 V; source gas: 50 L/min; entrance potential: 8 V; collision energy: 45; declustering potential: 45 V; column temperature: 50 °C; Q1 resolution: high; Q3 resolution: unit). The transitions monitored (324→252 for **1**, 322→292 for **2**) were based on published tandem MS spectra[7,30].

LC–TOF–HRMS was performed on an Agilent 1200 series Rapid Resolution HPLC system. Mobile phases were the same as above. 2 µL of sample was injected onto a Phenomenex Kinetex XB-C18 (3 mm × 50 mm) column. Method: 30% B for 8 min, ramp from 30% to 80% B in 20 min, 80% B for 4 min, ramp to 35% B in 1 min, re-equilibrate at 30% B for 7 min; all at a flow rate: 200 µL/min. An Agilent ESI source was used in the positive ion mode

(drying gas: 11 L/min, temperature: 325 °C, capillary voltage: 3,500 V, nebulizer gas: 25 lb/in^2, fragmentor: 150 V, skimmer: 50 V, declustering potential: 45 V, column temperature: 50 °C, OCT 1 RF Vpp: 170 V).

Semi-quantitative shotgun proteomics. Cell lysis and protein precipitation were performed using a chloroform–methanol extraction as previously described[31]. The protein pellet was resuspended in 100 mM (NH$_4$)HCO$_3$ with 20% methanol and the protein concentration was measured using the DC Protein Assay Kit (Bio-Rad). The protein was reduced with 5 mM TCEP for 30 min at room temperature, alkylated with 10 mM iodoacetamide for 30 min in the dark at room temperature, and digested with trypsin (1:50 w/w, trypsin:protein) overnight at 37 °C.

Peptide samples (20 µg) were analyzed on an Agilent 6550 iFunnel Q-TOF mass spectrometer coupled to an Agilent 1290 UHPLC system (Agilent Technologies). Peptides were loaded into an Ascentis Express Peptide ES-C18 column (100 mm × 2.1 mm i.d., 2.7-µm particle size; Sigma-Aldrich, St. Louis, MO, USA) operating at 60 °C and flowing at 0.400 mL/min. Mobile phase: A = 0.1% formic acid in water; B = 0.1% formic acid in acetonitrile. Method: 2% B for 2 min, ramp from 2% to 30% B over 30 min, ramp to 50% over 5 min, ramp to 80% over 1 min, hold at 80% B for 7 min, ramp to 2% B over 1 min, hold at 2% B for 4 min. An Agilent Dual Jet Stream Electrospray Ionization source was used in positive-ion mode. Gas temperature: 250 °C, drying gas: 14 L/min, nebulizer: 35 psig, sheath gas temp: 250 °C, sheath gas flow: 11 L/min, VCap: 4,500 V, nozzle voltage: 1,000 V, fragmentor: 180 V, and OCT 1 RF Vpp: 750 V.

The data were acquired with Agilent MassHunter Workstation version B.06.01 and searched against the *P. rubra* genome using Mascot version 2.3.02 (Matrix Science), then filtered and refined using Scaffold version 4.6.1 (Proteome Software, Inc.).

Bioinformatics. Pre-aligned Uniprot-RP75 (representative proteome clustered at 75% sequence identity) sequences for the FA hydroxylase (PF04116) family were obtained directly from Pfam version 3.0 (ref. 32). A maximum-likelihood phylogenetic tree was built with FastTree using default parameters[33]. Branches were assigned colors based on metadata from the UniProt database[34]. The tree was rendered using iTOL version 3 (ref. 35).

Data availability. Strains and plasmids developed for this study (**Supplementary Tables 4** and **5**), along with annotated sequences, have been deposited in the public instance of the Joint BioEnergy Institute Registry (https://public-registry.jbei.org/folders/260) and are physically available from the authors and/or Addgene (http://www.addgene.org) upon reasonable request. The Department of Energy will provide public access to these results of federally sponsored research in accordance with the DOE Public Access Plan (http://energy.gov/downloads/doe-public-access-plan).

A **Life Sciences Reporting Summary** for this paper is available.

26. Johnson, R.E., de Rond, T., Lindsay, V.N.G., Keasling, J.D. & Sarpong, R. *Org. Lett.* **17**, 3474–3477 (2015).
27. Dairi, K., Tripathy, S., Attardo, G. & Lavallée, J.-F. *Tetrahedr. Lett.* **47**, 2605–2606 (2006).
28. Hillson, N.J., Rosengarten, R.D. & Keasling, J.D. *ACS Synth. Biol.* **1**, 14–21 (2012).
29. Wang, P. *et al. Microb. Cell Fact.* **14**, 11 (2015).
30. Alihosseini, F., Lango, J., Ju, K.-S., Hammock, B.D. & Sun, G. *Biotechnol. Prog.* **26**, 352–360 (2010).
31. Batth, T.S., Keasling, J.D. & Petzold, C.J. *Methods Mol. Biol.* **944**, 237–249 (2012).
32. Finn, R.D. *et al. Nucleic Acids Res.* **42**, D222–D230 (2014).
33. Price, M.N., Dehal, P.S. & Arkin, A.P. *Mol. Biol. Evol.* **26**, 1641–1650 (2009).
34. UniProt Consortium. *Nucleic Acids Res.* **43**, D204–D212 (2015).
35. Letunic, I. & Bork, P. *Nucleic Acids Res.* **44**, W242–W245 (2016).

nature research

Corresponding author(s):   Tristan de Rond

☐ Initial submission   ☐ Revised version   ☒ Final submission

Life Sciences Reporting Summary

Nature Research wishes to improve the reproducibility of the work that we publish. This form is intended for publication with all accepted life science papers and provides structure for consistency and transparency in reporting. Every life science submission will use this form; some list items might not apply to an individual manuscript, but all fields must be completed for clarity.

For further information on the points included in this form, see Reporting Life Sciences Research. For further information on Nature Research policies, including our data availability policy, see Authors & Referees and the Editorial Policy Checklist.

Experimental design

Sample size

Describe how sample size was determined.

> For the enzyme kinetics in Figure 2b, N=3. This is enough to highlight the qualitative results shown in this figure.

Data exclusions

Describe any data exclusions.

> no data was excluded

Replication

Describe whether the experimental findings were reliably reproduced.

> all attempts at replication were successful

Randomization

Describe how samples/organisms/participants were allocated into experimental groups.

> N/A

Blinding

Describe whether the investigators were blinded to group allocation during data collection and/or analysis.

> N/A

Note: all studies involving animals and/or human research participants must disclose whether blinding and randomization were used.

Statistical parameters

For all figures and tables that use statistical methods, confirm that the following items are present in relevant figure legends (or in the Methods section if additional space is needed).

n/a	Confirmed	
☒	☐	The exact sample size (*n*) for each experimental group/condition, given as a discrete number and unit of measurement (animals, litters, cultures, etc.)
☒	☐	A description of how samples were collected, noting whether measurements were taken from distinct samples or whether the same sample was measured repeatedly
☒	☐	A statement indicating how many times each experiment was replicated
☒	☐	The statistical test(s) used and whether they are one- or two-sided (note: only common tests should be described solely by name; more complex techniques should be described in the Methods section)
☒	☐	A description of any assumptions or corrections, such as an adjustment for multiple comparisons
☒	☐	The test results (e.g. *P* values) given as exact values whenever possible and with confidence intervals noted
☒	☐	A clear description of statistics including central tendency (e.g. median, mean) and variation (e.g. standard deviation, interquartile range)
☐	☒	Clearly defined error bars

See the web collection on statistics for biologists for further resources and guidance.

▶ Software

Policy information about availability of computer code

7. Software

Describe the software used to analyze the data in this study.

> All the software used is mentioned in the methods section.

For manuscripts utilizing custom algorithms or software that are central to the paper but not yet described in the published literature, software must be made available to editors and reviewers upon request. We strongly encourage code deposition in a community repository (e.g. GitHub). *Nature Methods* guidance for providing algorithms and software for publication provides further information on this topic.

▶ Materials and reagents

Policy information about availability of materials

8. Materials availability

Indicate whether there are restrictions on availability of unique materials or if these materials are only available for distribution by a for-profit company.

> All materials are readily available from the authors

Antibodies

Describe the antibodies used and how they were validated for use in the system under study (i.e. assay and species).

> N/A

10. Eukaryotic cell lines

a. State the source of each eukaryotic cell line used.

> N/A

b. Describe the method of cell line authentication used.

> N/A

c. Report whether the cell lines were tested for mycoplasma contamination.

> N/A

d. If any of the cell lines used are listed in the database of commonly misidentified cell lines maintained by ICLAC, provide a scientific rationale for their use.

> N/A

Animals and human research participants

Policy information about studies involving animals; when reporting animal research, follow the ARRIVE guidelines

11. Description of research animals

Provide details on animals and/or animal-derived materials used in the study.

> N/A

Policy information about studies involving human research participants

12. Description of human research participants

Describe the covariate-relevant population characteristics of the human research participants.

> N/A